bioRxiv preprint doi: https://doi.org/10.1101/067520; this version posted October 24, 2016. The copyright holder for this preprint (which was not certified by peer review) is the author/funder, who has granted bioRxiv a license to display the preprint in perpetuity. It is made available under aCC-BY-NC-ND 4.0 International license.

# Divergent heteroblastic trajectories underlie disparate leaf shapes among *Passiflora* species

Daniel H. Chitwood[1, §] and Wagner C. Otoni[2, §]

[1]Donald Danforth Plant Science Center, St. Louis, MO USA

[2]Departamento de Biologia Vegetal/BIOAGRO, Universidade Federal de Viçosa, Viçosa, MG, Brasil

**Keywords**: *Passiflora*, morphometrics, leaves, leaf shape, leaf morphology, heteroblasty, Procrustes analysis, landmarks, Elliptical Fourier Descriptors

[§]To whom correspondence should be addressed:

Daniel H. Chitwood
Donald Danforth Plant Science Center
975 North Warson Road
St. Louis, MO 63132
Phone: (314) 587-1609
Fax: (314) 587-1709
e-mail:
dchitwood@danforthcenter.org

Wagner C. Otoni
Departamento de Biologia
Vegetal/BIOAGRO
Universidade Federal de Viçosa
36570-900 Viçosa, MG, Brasil
Phone: +55 (31) 3899 2930
e-mail: wotoni@ufv.br

bioRxiv preprint doi: https://doi.org/10.1101/067520; this version posted October 24, 2016. The copyright holder for this preprint (which was not certified by peer review) is the author/funder, who has granted bioRxiv a license to display the preprint in perpetuity. It is made available under aCC-BY-NC-ND 4.0 International license.

## Abstract

BACKGROUND: Not only does leaf shape vary between *Passiflora* species, but between sequential nodes of the vine. The often profound changes in leaf shape within *Passiflora* vines reflect the temporal development of the shoot apical meristem from which leaves are derived and patterned, a phenomenon known as heteroblasty.

METHODS: Here, we continue a morphometric analysis of more than 3,300 leaves from 40 different *Passiflora* species using two different methods: homologous landmarks and Elliptical Fourier Descriptors (EFDs).

RESULTS: Changes in leaf shape across the vine are first quantified in allometric terms; that is, changes in the relative area of leaf sub-regions expressed in terms of overall leaf area. The ability of different nodes to predictively discriminate species and the variability of landmark and EFD traits at each node is then analyzed. Heteroblastic trajectories, the changes in leaf shape between the first and last measured leaves in a vine, are then compared between species in a multivariate space.

DISCUSSION: Leaf shape diversity among *Passiflora* species is expressed in a heteroblastic-dependent manner. Leaf shape between species and across the heteroblastic series is constrained by allometric relationships. The first leaves in the series are not only more similar to each other, but are also less variable across species. From this similar, shared leaf shape, subsequent leaves in the heteroblastic series follow divergent morphological trajectories, creating the disparate shapes characteristic of *Passiflora* leaf shape diversity.

## Introduction

bioRxiv preprint doi: https://doi.org/10.1101/067520; this version posted October 24, 2016. The copyright holder for this preprint (which was not certified by peer review) is the author/funder, who has granted bioRxiv a license to display the preprint in perpetuity. It is made available under aCC-BY-NC-ND 4.0 International license.

In the companion piece to this manuscript, we describe the profound diversity in leaf shape between *Passiflora* species (Chitwood and Otoni, 2016), but leaves also change shape over the lifetime of a single plant. Heteroblasty is a phenomenon that results from the temporal development of the shoot apical meristem, creating successive changes in the traits of the lateral organs it produces at each node, including the shapes of leaves. Johann Wolfgang von Goethe described the transformation in leaf shape across a shoot as a "metamorphosis", correctly suggesting that lateral organs are serially homologous structures, from the juvenile and adult leaf shapes a plant displays during vegetative development to reproductive organs (Goethe, 1952; Friedman and Diggle, 2011; Chitwood and Sinha, 2014). There have been many hypotheses about the origins of heteroblastic changes in leaf shape. Inspired by Ernst Haeckel, it was hypothesized that juvenile leaf shapes represented the ancestral condition, and that adult leaves were derived leaf forms (Cushman, 1902; Cushman, 1903). In parallel, another school of thought led by Karl Goebel favored a more environmental explanation for heteroblasty: only supported by the photosynthesis of cotyledons and young leaves, the shape of juvenile leaves represented the aborted development of mature leaf morphology (Goebel, 1908). Careful morphological analysis of young leaf primordia refutes such an idea in Cucurbits (Jones, 1992; Jones, 1995), but classical (Allsopp, 1953a; Allsopp, 1953b; Allsopp, 1954; Njoku, 1956; Njoku, 1971; Roebbelen, 1957; Feldman and Cutter, 1970) and molecular experiments (Yang et al., 2013; Yu et al., 2013) in other species suggest that sugar can serve as a signal hastening the heteroblastic series.

*Passiflora* species exhibit dramatic heteroblastic changes in leaf shape (**Fig. 1**). *Passiflora edulis* begins with an ellipsoid leaf shape, that transitions to a tri-lobed leaf later in the series (**Fig. 1A**). Like *P. edulis*, *P. caerulea* leaves begin ellipsoid, but transition to a highly dissected tri-lobe leaf morph and then to four- and five-lobed leaves, and even seven-lobed leaves, as previously reported (Allsopp, 1967) and observed by the authors. Sometimes the transition to lobed leaves is erratic, as in *P. racemosa*, in which the lobes manifest asymmetrically or can revert back to the

bioRxiv preprint doi: https://doi.org/10.1101/067520; this version posted October 24, 2016. The copyright holder for this preprint (which was not certified by peer review) is the author/funder, who has granted bioRxiv a license to display the preprint in perpetuity. It is made available under aCC-BY-NC-ND 4.0 International license.

juvenile form with no lobes later in the leaf series (**Fig. 1A**). Other *Passiflora* species exhibit variable degrees of heteroblastic changes in leaf shape (**Fig. 1B**). Unlike the generalized theories of heteroblastic changes in leaf shape inspired by Haeckel or put forth by Goebel, a specific hypothesis has been proposed for the dramatic changes in leaf shape observed in *Passiflora*. Just as diversity in leaf shape among *Passiflora* species is hypothesized to result from diversifying selective pressure from egg-laying *Heliconius* butterflies using leaf shape as a cue (Klucking, 1992; MacDougal, 1994; Gilbert, 1975; Dell'aglio, 2016) diverse leaf shapes in a single vine, resulting from heteroblasty, are thought to similarly deceive butterflies by mimicking non-host plants during critical stages of the vine lifecycle (Gilbert, 1982).

Morphometric approaches are critical to separating shape attributes that differentiate species (or genotypes, in genetic studies) regardless of developmental context (Chitwood et al., 2013; Chitwood et al., 2014a) versus purely heteroblastic changes in leaf shape (Chitwood et al., 2012; Chitwood et al., 2016a). The genetic basis of natural variation in heteroblastic shape change can also be measured (Chitwood et al., 2014b). The shape features that vary between species are often distinct from those that differentiate leaves arising from sequential nodes, such that using discriminant analyses, species identity can be predicted regardless of node position and vice versa (Chitwood et al., 2016a; Chitwood et al., 2016b). This result is also true among *Passiflora* species (Chitwood and Otoni, 2016), demonstrating distinct contributions of species identity and heteroblasty to the shape of each leaf.

Here, we continue an analysis of more than 3,300 leaves from 40 *Passiflora* species (Chitwood and Otoni, 2016) but focus on heteroblastic changes in leaf shape. Leaf shape changes across the heteroblastic series are allometrically constrained, but these allometric constraints vary between species. Discriminant analysis of shape features capable of predicting species identity for leaves at each node demonstrates that leaves arising from the first nodes at the base of the vine are more similar to each other and more easily confused between species. The similarity in shape between leaves arising from early nodes between species is supported by an

bioRxiv preprint doi: https://doi.org/10.1101/067520; this version posted October 24, 2016. The copyright holder for this preprint (which was not certified by peer review) is the author/funder, who has granted bioRxiv a license to display the preprint in perpetuity. It is made available under aCC-BY-NC-ND 4.0 International license.

observed lack of variability in juvenile compared to adult leaves. Analysis of changes in shape between the first and last leaves of a vine in a multivariate space suggest that juvenile leaves between species arise within a common region of morphospace. The diversity of leaf shapes observed among *Passiflora* species arises from divergent heteroblastic changes in leaf shape away from the shared juvenile leaf form.

## Materials and Methods

### *Data Description*

The differences in leaf shape between species arise through changes in leaves arising from successive nodes within a single vine, the result of the temporal development of the shoot apical meristem known as heteroblasty. How heteroblastic changes in leaf shape contribute to diversity among *Passiflora* species is the focus of this manuscript. By providing code and the raw data used in analyses, this manuscript also serves as a tutorial to leaf morphometrics, using both landmark and Elliptical Fourier Descriptor (EFD) methods.

A dataset released with the companion manuscript (Chitwood and Otoni, 2016) consists of 555 scans of leaves from 40 different species of *Passiflora* in which the order of leaves arising from the vine is recorded (starting with "1" for the youngest leaf scanned from the growing tip of each vine). We importantly note: the numbering of nodes in the raw scans described above, starting at the tip of the shoot, is opposite from the numbering of nodes presented in the manuscript, in which numbering (starting with "1") begins with the oldest leaf at the base of the shoot. The reason for this opposite numbering in the manuscript is that by beginning the counting of nodes with "1" at the shoot base the numbering aligns with the heteroblastic series (which begins with the first emerged leaf at the shoot base).

bioRxiv preprint doi: https://doi.org/10.1101/067520; this version posted October 24, 2016. The copyright holder for this preprint (which was not certified by peer review) is the author/funder, who has granted bioRxiv a license to display the preprint in perpetuity. It is made available under aCC-BY-NC-ND 4.0 International license.

Data from more than 3,300 leaves, and the code to analyze the data and reproduce the figures in this manuscript, are provided, including both landmark data, measuring the vasculature, lobes, and sinuses, and Elliptical Fourier Descriptor (EFD) data, which quantifies leaf outlines (Chitwood, 2016). It is hoped that the release of this data and code will assist others in developing novel morphometric approaches to better understand the genetic, developmental, and environmental basis of leaf shape. Data and code used in the companion manuscript (Chitwood and Otoni, 2016) is provided along with the data and code used in the analysis of this manuscript (Chitwood, 2016).

*Plant materials and growth conditions*

*Passiflora* germplasm was kindly provided by R. Silva (Viveiros Flora Brasil, Araguari, MG, Brazil), Dr. F.G. Faleiro (EMBRAPA Cerrados, Planaltina, DF, Brazil), Prof. M.M. Souza (Universidade Estadual de Santa Cruz - UESC, Ilhéus, BA, Brazil), M. Peixoto (Mogi das Cruzes, SP, Brazil), Prof. M.L. Silva (Universidade do Estado de Mato Grosso, Tangará da Serra, MT, Brazil), and Prof. C.H. Bruckner (Universidade Federal de Viçosa, Viçosa, MG, Brazil).

The plants were germinated from seed, planted between late October 2015 and early March 2016, in Viçosa, at the Federal University of Viçosa, MG, Brazil. The populations were raised and maintained under polycarbonate-covered greenhouse conditions, equipped with automatic environmental control using exhaust fans and evaporative cooling panels (with expanded clay wettable pads). Seeds for each *Passiflora* species were sown in 128 cell propagation plastic trays (GPlan Comércio de Produtos Agrícola s EIRELI – ME, São Paulo, SP, Brazil) filled with horticultural organic Tropstrato HT Hortaliças substrate (Vida Verde Indústria e Comércio de Insumos Orgânicos Ltda, Mogi Mirim, SP, Brazil). After germination (30-40 days), plantlets were individually transplanted to 5 L capacity plastic pots (EME-A-EME Ind. Com. Ltda., Petrópolis, RJ, Brazil) filled with horticultural substrate. Each pot received 5 g of Osmocote® Plus NPK 15-09-12 3-4 month controlled release

bioRxiv preprint doi: https://doi.org/10.1101/067520; this version posted October 24, 2016. The copyright holder for this preprint (which was not certified by peer review) is the author/funder, who has granted bioRxiv a license to display the preprint in perpetuity. It is made available under aCC-BY-NC-ND 4.0 International license.

fertilizer (Scotts, USA). Plants were irrigated on a daily-basis with tap water, and no phytosanitary control was applied.

For scanning, a multifunction printer (Canon PIXMA MX340 Wireless Office All-in-One Printer, model 4204B019, USA) was used. A 20 cm metallic ruler was positioned at the bottom of each scanned sheet as a size marker. Leaves were carefully detached, from the base to the tip of the shoot, and affixed to an A4 paper sheet, adaxial face down, using 12 mm-double sided tape (Scotch Model 9400, 3M do Brasil, SP, Brazil). The numbers written near each leaf indicate position in the shoot, in a tip-to-base direction, starting with the youngest leaf at the tip of the shoot.

*Morphometric and statistical analyses*

All morphometric data and code used for statistical analysis is available on GitHub (Chitwood, 2016). Landmarks, as described in the text, were placed on leaves in ImageJ (Abramoff, Magalhaes, and Ram, 2004). Procrustes superimposition was performed using the shapes package (Dryden, 2015) in R (R Development Core Team, 2016) with the procGPA function using reflect=TRUE.

To isolate outlines for Elliptical Fourier Descriptor (EFD) analysis, the "Make Binary" function in ImageJ (Abramoff, Magalhaes, and Ram, 2004) was found to be sufficient to segment leaves. The wand tool was used to select individual binary leaf outlines, which were pasted into a new canvas, which was subsequently saved as an individual image, which was named by vine and node position from which the leaf was derived. The binary images were batch converted into RGB .bmp files and read into SHAPE, which was used to perform chain-code analysis (Iwata et al., 1998; Iwata and Ukai, 2002). The resulting chain-code .chc file was then used to calculate normalized EFDs. The resulting normalized EFD .nef file was then read into Momocs (version 0.2-6) (Bonhomme et al., 2014) in R. The harmonic contributions to shape

bioRxiv preprint doi: https://doi.org/10.1101/067520; this version posted October 24, 2016. The copyright holder for this preprint (which was not certified by peer review) is the author/funder, who has granted bioRxiv a license to display the preprint in perpetuity. It is made available under aCC-BY-NC-ND 4.0 International license.

were visualized using the hcontrib function. Averaged leaf outlines were calculated using the meanShapes function.

Unless otherwise noted, all visualization was performed using ggplot2 in R (Wickham, 2009). Linear Discriminant Analysis (LDA) was performed using the lda function and subsequent prediction of species identity or heteroblastic node position performed using the predict function with MASS (Venables and Ripley, 2002). For prediction, LDA was performed with CV="TRUE", which is a "leave one out" cross-validation approach in which for each leaf an LDA is performed excluding the leaf after which it is assigned to the resulting LDA space it was excluded from. Hierarchical clustering was performed using the hclust function. t-distributed Stochastic Neighbor Embedding (t-SNE) was performed using the Rtsne package (Krijthe, 2015) in R with perplexity=40.

## Results

### *Heteroblastic changes in Passiflora leaf shape*

The greater than 3,300 leaves analyzed in this study come from 40 different species of *Passiflora* and were collected in order from the base of the vine onwards to the growing tip, keeping track of the node from which each leaf originated. Among the 40 *Passiflora* species sampled, the degree of heteroblastic shape change is variable (**Fig. 1**). In the companion manuscript (Chitwood and Otoni, 2016), we defined seven species groups (classes) based on their clustering in a Principal Component Analysis (PCA) and qualitative shape differences. Members of Class G, with lance-shaped leaves, generally exhibit little to no changes in leaf shape across the leaf series, and similarly Class E leaves remain round regardless of shoot position. Members of Class C and D, which are characterized by different numbers of lobes later in the series, begin with a rounder, less lobed juvenile leaf shape at the base of the vine. Members of Class A and B, with wide "bat-like" leaves begin with a rounder leaf shape that transitions to a stereotypical wide leaf (**Fig. 1**).

bioRxiv preprint doi: https://doi.org/10.1101/067520; this version posted October 24, 2016. The copyright holder for this preprint (which was not certified by peer review) is the author/funder, who has granted bioRxiv a license to display the preprint in perpetuity. It is made available under aCC-BY-NC-ND 4.0 International license.

Generally, if heteroblastic changes in leaf shape are observed, the juvenile leaf form (at the base of the shoot) tends to be rounder and exhibit less lobing compared to adult leaves at the shoot tip (**Fig. 1B**). To substantiate this statement, we used 15 landmarks measuring vascular patterning and the position of the lobes and sinuses, and Elliptical Fourier Descriptors (EFDs), quantifying the contours of leaves, to visualize shape changes through the heteroblastic series (**Fig. 2A-B**, as described in the companion manuscript; Chitwood and Otoni, 2016). Averaged landmarked leaves (**Fig. 2C-D**) and EFD-derived outlines (**Fig. 2E**) across the leaf series compared to the first leaf show that leaves become progressively more dissected. However, most of these heteroblastic changes occur between leaves 1 and 2 at the shoot base, and the remainder of leaves later in the shoot, on average, shows little further changes in shape. This result is consistent with the observation in the companion manuscript (Chitwood and Otoni, 2016) that shape features in juvenile leaves in the first nodes allow them to be correctly assigned to the predicted node at higher rates than leaves later in the series. We return to this idea later, and explore the hypothesis that across species juvenile leaves are more similar to each other than leaves later in the series that exhibit divergent shapes.

*Allometric changes in leaf shape across the heteroblastic series*

To explore the relative contributions of leaf sub-areas to differences in leaf shape across the heteroblastic leaf series in different species, we performed an allometric analysis. Changes in leaf shape, whether between species or within the heteroblastic series, often correlate linearly with size (Chitwood et al., 2016b); whether such relationships exist in this dataset remains an open question. Procrustes-aligned leaves were divided into sub-regions (**Fig. 2F**), including the areas of the midvein and proximal vein, and distal and proximal leaf blade areas. The rationale of using Procrustes-aligned leaf shapes (which have been scaled, translated, and rotated to superimpose leaves for analysis) is to analyze the relative contributions of vein and blade area to total leaf area. When plotting the square root of each sub-region area

bioRxiv preprint doi: https://doi.org/10.1101/067520; this version posted October 24, 2016. The copyright holder for this preprint (which was not certified by peer review) is the author/funder, who has granted bioRxiv a license to display the preprint in perpetuity. It is made available under aCC-BY-NC-ND 4.0 International license.

against the square root of the overall Procrustes-aligned leaf area, clear linear relationships are observed (**Fig. 2G**). Notably, blade areas expand at a higher rate compared to vein areas as the total leaf area increases (that is, the slope of the blade sub-regions is greater than the vein sub-regions). That total area of the leaf occupied by blade expands at a faster rate than the area occupied by veins is consistent with the previous results observed in grapevines (Chitwood et al., 2016a; Chitwood et al., 2016b).

When the results are plotted for each species, the general trend of blade area expanding at the expense of vein area is observed, but there is a large amount of variation between species (**Fig. 3**). For example, *P. misera* exhibits fairly linear relationships in which both blade regions have similar slopes that are greater than the vein regions. Contrastingly, the distribution of total leaf area for *P. caerulea* is bimodal, and differences in each population of leaves contributes to widely different slopes between the distal and proximal blade sub-regions. The distinctness of each *P. caerulea* sub-population reflects the discrete transformation of leaf shape from entire to highly dissected and palmate (**Fig. 1A**). This is reflected when the heteroblastic node number is projected onto the plots (**Fig. 4**), revealing distinct populations of juvenile and adult leaves with different ratios of blade and vein areas that contribute to each leaf type. Other species vary in the extent that the heteroblastic series is defined by the linear allometric relationships contributing to differences in leaf shape across the leaf series.

Although overall blade sub-regions expand at faster rates compared to vein sub-regions, and this relationship is mostly linear across all species (**Fig. 2G**), species vary widely in the relative ratios of these regions across allometric lines (**Fig. 3**) and the heteroblastic series (**Fig. 4**).

*Divergent heteroblastic trajectories and similar juvenile leaf shapes*

bioRxiv preprint doi: https://doi.org/10.1101/067520; this version posted October 24, 2016. The copyright holder for this preprint (which was not certified by peer review) is the author/funder, who has granted bioRxiv a license to display the preprint in perpetuity. It is made available under aCC-BY-NC-ND 4.0 International license.

A number of pieces of evidence suggest the earliest leaf shapes in the heteroblastic series are similar across *Passiflora* species, and that leaves later in the series differ between species. In the companion manuscript (Chitwood and Otoni, 2016), the first two juvenile leaves of the series were assigned to the correct predicted node at higher rates compared to later leaves in the series, suggesting these leaves are similar across species. When the average shape of leaves across the heteroblastic series are compared using landmarks (**Fig. 2D**) and contours derived from Elliptical Fourier Descriptors (EFDs) (**Fig. 2E**) it is evident that the more lobed leaf shape characteristic of later leaves is achieved within the first two nodes.

To test the idea that juvenile leaves at the base of the shoot are more similar between species than those later in the series, we performed a Linear Discriminant Analysis (LDA) using both landmark and EFDs to discriminate leaves from each node by species identity (**Fig. 5A**). Although there is wide variability of the ability to discriminate the leaves of each species, the LDAs using leaves from nodes 1 and 2 performed poorly in their ability to discriminate leaves by species compared to subsequent nodes. From the overall average correct reassignment rate for the LDA performed for each node (see bottom of **Fig. 5A**) it is evident that leaves from nodes 1 and 2 have less distinctive features differentiating leaves from species compared to later nodes. This suggests that leaves from nodes 1 and 2 are more similar in shape between species than leaves from later nodes.

A more direct test of variability in leaf shape is to measure the standard deviation of the raw traits used to measure leaf shape. Shape features of the leaf were hierarchically clustered (as described in the companion manuscript; Chitwood and Otoni, 2016) and the standard deviation for each across species for each node calculated (**Fig. 5B**). The majority of shape features either have reduced or unchanged standard deviation values in the first 1-3 leaves of the series compared to later leaves. A minority of shape features, especially the x coordinate values for landmarks defining the petiolar junction and bases of the major veins (landmarks 1-6) have increased standard deviation values in the earlier nodes. The results suggest

bioRxiv preprint doi: https://doi.org/10.1101/067520; this version posted October 24, 2016. The copyright holder for this preprint (which was not certified by peer review) is the author/funder, who has granted bioRxiv a license to display the preprint in perpetuity. It is made available under aCC-BY-NC-ND 4.0 International license.

that generally leaf shape is less variable in leaves from the first nodes (**Fig. 5B**) consistent with the observation that juvenile leaves discriminate species less than leaves later in the series (**Fig. 5A**). Exceptionally, the landmarks defining the petiolar junction in the x coordinate direction are more variable in juvenile than adult leaves (**Fig. 5B**).

To visualize the divergent heteroblastic trajectories leading to disparate leaf shapes between *Passiflora* species, we used a t-distributed Stochastic Neighbor Embedding (t-SNE) approach to reduce the dimensionality of the data (**Fig. 6A**) (Krijthe, 2015). t-SNE separates species classes similarly to the Principal Component Analysis (PCA) performed in the companion manuscript (Chitwood and Otoni, 2016) and benefits from no assumptions of linearity and reducing the data to strictly two dimensions. By doing so, each sampled vine can be visualized as a vector in the two dimensional space, with the base and tip of the vector corresponding to the first sampled node at the base of the shoot and the furthest sampled node at the tip of the shoot, respectively (**Fig. 6B**). Each vector, therefore, is a representation of the shape space traversed over the heteroblastic series.

The bases of the vectors representing each vine tend to cluster together, with similar Dimension 1 values but varying across Dimension 2. From this common region representing a shared juvenile leaf shape, the directions of each vector for different species classes vary, representing differing heteroblastic trajectories leading to disparate adult leaf shapes at nodes towards the shoot tips. To better visualize the divergent heteroblastic trajectories of each species class, each vector base was centered to the origin (**Fig. 6C**). After centering, it is apparent that different species classes vary drastically—sometimes diametrically opposed—in the direction of their heteroblastic shape changes.

Collectively, the inability of leaves from the first nodes to successfully discriminate different species (**Fig. 5A**), the reduced variability in shape features of leaves from the first nodes (**Fig. 5B**), and the divergent heteroblastic trajectories between

bioRxiv preprint doi: https://doi.org/10.1101/067520; this version posted October 24, 2016. The copyright holder for this preprint (which was not certified by peer review) is the author/funder, who has granted bioRxiv a license to display the preprint in perpetuity. It is made available under aCC-BY-NC-ND 4.0 International license.

species classes (**Fig. 6**) demonstrate that juvenile leaves between *Passiflora* species are similar and that divergent heteroblastic trajectories are responsible for the distinctive leaf shapes between species.

## Discussion and Conclusions

A number of explanations for heteroblasty, the changes in leaf shape and other traits across a shoot resulting from the temporal development of the shoot apical meristem from which lateral organs arise, have been proposed. The idea that juvenile and adult leaves recapitulate the ancestral and derived leaf forms across evolution (Cushman, 1902; Cushman, 1903) or that juvenile leaves result from the lack of photosynthate to complete development (Goebel, 1908) have been proposed as possible explanations for the sometimes dramatic changes in leaf shape across a shoot. In *Passiflora*, the heteroblastic series has been hypothesized to be a mechanism to avoid *Heliconius* butterflies that use leaf shape as a cue to lay eggs (Gilbert, 1982). Although we cannot distinguish between these alternatives, our morphometric data does reveal how leaf shape changes manifest across vines and contribute to diversity within the genus *Passiflora* (**Fig. 1**). Heteroblastic changes in leaf shape are allometrically constrained to linear relationships that vary between species (**Figs. 2-4**). Juvenile leaves are more often mistakenly identified between species than adult leaves found later in the shoot (**Fig. 5A**), and consistent with juvenile leaves resembling each other, the variability of most morphometric features is lower in juvenile compared to adult leaves (**Fig. 5B**). Comparing the first and last leaves of a shoot within a multivariate space, the heteroblastic trajectories of different species are divergent, originating from a similar juvenile form but traversing towards disparate shapes (**Fig. 6**). Our data show that the striking differences in leaf shape between *Passiflora* species are expressed in a developmental manner, later in the heteroblastic series.

## Funding statement

bioRxiv preprint doi: https://doi.org/10.1101/067520; this version posted October 24, 2016. The copyright holder for this preprint (which was not certified by peer review) is the author/funder, who has granted bioRxiv a license to display the preprint in perpetuity. It is made available under aCC-BY-NC-ND 4.0 International license.

Brazilian sponsoring agencies, namely FAPEMIG (Grant no. CBB - APQ-01131-15), CNPq (Grant no. 459.529/2014-5) and CAPES, are acknowledged for financial support.

## Authors' contributions

The overall project was conceived by DHC and WCO. WCO grew and scanned all plant material and DHC carried out analysis. DHC and WCO wrote the paper.

## Competing interests

The authors declare that they have no competing interests.

## References

Abràmoff MD, Magalhães PJ, Ram SJ. Image processing with ImageJ. Biophotonics international. 2004;11(7):36-42.

Allsopp A. Experimental and analytical studies of pteridophytes XIX. Investigations on Marsilea 2. Induced reversion to juvenile stages. Ann Bot. 1953a;17:37-55.

Allsopp A. Experimental and analytical studies of pteridophytes XXI. Investigations on Marsilea 3. The effect of various sugars on development and morphology. Ann Bot. 1953b;17:447-463.

Allsopp A. Juvenile stages of plants and the nutritional status of the shoot apex. Nature. 1954;173:1032-1035.

Allsopp A. Heteroblastic development in vascular plants. Advances in morphogenesis. 1967;6:127-171.

Bonhomme V, Picq S, Gaucherel C, Claude J. Momocs: outline analysis using R. Journal of Statistical Software. 2014;56:1-24.

Chitwood DH, Headland LR, Kumar R, Peng J, Maloof JN, Sinha NR. The developmental trajectory of leaflet morphology in wild tomato species. Plant Physiol. 2012;158:1230-40.

bioRxiv preprint doi: https://doi.org/10.1101/067520; this version posted October 24, 2016. The copyright holder for this preprint (which was not certified by peer review) is the author/funder, who has granted bioRxiv a license to display the preprint in perpetuity. It is made available under aCC-BY-NC-ND 4.0 International license.

Chitwood DH, Kumar R, Headland LR, Ranjan A, Covington MF, Ichihashi Y, Fulop D, Jimenez-Gomez JM, Peng J, Maloof JN, Sinha NR. A quantitative genetic basis for leaf morphology in a set of precisely defined tomato introgression lines. Plant Cell. 2013;25:2465-81.

Chitwood DH, Sinha NR. Plant Development: Small RNAs and the Metamorphosis of Leaves. Current Biology. 2014;24:R1087-R1089.

Chitwood DH, Ranjan A, Martinez CC, Headland LR, Thiem T, Kumar R, Covington MF, Hatcher T, Naylor DT, Zimmerman S, Downs N, Raymundo N, Buckler ES, Maloof JN, Aradhya M, Prins B, Li L, Myles S, Sinha NR. A modern ampelography: a genetic basis for leaf shape and venation patterning in grape. Plant Physiol. 2014a;164:259-72.

Chitwood DH, Ranjan A, Kumar R, Ichihashi Y, Zumstein K, Headland LR, Ostria-Gallardo E, Aguilar-Martinez JA, Bush S, Carriedo L, Fulop D, Martinez CC, Peng J, Maloof JN, Sinha NR. Resolving distinct genetic regulators of tomato leaf shape within a heteroblastic and ontogenetic context. Plant Cell. 2014b;26:3616-29.

Chitwood DH. PassifloraLeaves. GitHub. 2016. https://github.com/DanChitwood/PassifloraLeaves

Chitwood DH, Otoni WC. Morphometric analysis *Passiflora* leaves: the relationship between landmarks of the vasculature and elliptical Fourier descriptors of the blade. bioRxiv. 2016;

Chitwood DH, Klein LL, O'Hanlon R, Chacko S, Greg M, Kitchen C, Miller AJ, Londo JP. Latent developmental and evolutionary shapes embedded within the grapevine leaf. New Phytol. 2016a;210:343-55.

Chitwood DH, Rundell SM, Li DY, Woodford QL, Yu TT, Lopez JR, Greenblatt D, Kang J, Londo JP. Climate and developmental plasticity: interannual variability in grapevine leaf morphology. Plant Physiol. 2016b;170:1480-91.

Cushman JA. Studies of localized stages of growth in some common New England plants. Am Nat. 1902;36:865-885.

Cushman JA. Studies of localized stages in some plants of the botanic gardens of Harvard University. Am Nat. 1903;37:243-259.

Dell'aglio DD, Losada ME, Jiggins CD. Butterfly learning and the diversification of plant leaf shape. Frontiers in Ecology and Evolution. 2016;4:81.

Dryden IL. shapes: Statistical Shape Analysis. R package version 1.1-11. 2015;https://CRAN.R-project.org/package=shapes

bioRxiv preprint doi: https://doi.org/10.1101/067520; this version posted October 24, 2016. The copyright holder for this preprint (which was not certified by peer review) is the author/funder, who has granted bioRxiv a license to display the preprint in perpetuity. It is made available under aCC-BY-NC-ND 4.0 International license.

Feldman LJ, Cutter EG. Regulation of leaf form in Centaurea solstitalis L. I. Leaf development on whole plants in sterile culture. Bot Gaz. 1970;131:31-39.

Friedman WE, Diggle PK. Charles Darwin and the origins of plant evolutionary developmental biology. Plant Cell. 2011;23:1194-207.

Gilbert LE. Ecological consequences of a coevolved mutualism between butterflies and plants. Coevolution of animals and plants. 1975;210-240.

Gilbert LE. The coevolution of a butterfly and a vine. Sci Amer. 1982;110-121.

Goebel K. Einleitung in die experimentelle Morphologie der Pflanzen. B.G. Teubner: Leipzig. 1908;

Goethe JW. Botanical Writings. Trans. B. Mueller, introduction C.J. Engard. Honolulu: University of Hawaii Press. 1952;

Iwata H, Niikura S, Matsuura S, Takano Y, Ukai Y. Evaluation of variation of root shape of Japanese radish (Raphanus sativus L.) based on image analysis using elliptic Fourier descriptors. Euphytica. 1998;102:143-9.

Iwata H, Ukai Y. SHAPE: a computer program package for quantitative evaluation of biological shapes based on elliptic Fourier descriptors. Journal of Heredity. 2002;93:384-385.

Jones CS. Comparative ontogeny of a wild cucurbit and its derived cultivar. Evolution. 1992;46:1827-1847.

Jones CS. Does shade prolong juvenile development? A morphological analysis of leaf shape changes in Cucurbita argyrosperma subsp. sororia (Cucurbitaceae). American Journal of Botany. 1995;82:346-359.

Klucking EP. Leaf venation patterns, vol. 6. 1992;Berlin: J. Cramer. Passifloraceae, 222-262.

Krijthe J. Rtsne: T-Distributed Stochastic Neighbor Embedding using Barnes-Hut Implementation. R package version 0.10. 2015;https://CRAN.R-project.org/package=Rtsne

MacDougal JM. Revision of Passiflora subgenus Decaloba section Pseudodysosmia (Passifloraceae). Syst Bot Monogr. 1994;41:1-146.

Njoku E. Studies in the morphogenesis of leaves XI. The effect of light intensity on leaf shape in Ipomea caerulea. New Phytol. 1956;55:91-110.

bioRxiv preprint doi: https://doi.org/10.1101/067520; this version posted October 24, 2016. The copyright holder for this preprint (which was not certified by peer review) is the author/funder, who has granted bioRxiv a license to display the preprint in perpetuity. It is made available under aCC-BY-NC-ND 4.0 International license.

Njoku E. Effect of sugars and applied chemicals on the heteroblastic development in Ipomoea purpurea grown in aseptic culture. Am J Bot. 1971;58:61-64.

R Development Core Team. R: A language and environment for statistical computing. R Foundation for Statistical Computing, Vienna, Austria. 2016;http://www.R-project.org.

Roebbelen G. Uber Heterophyllie bei Arabidopsis thaliana (L.) Heynh. Ber Dtsch Bot Ges. 1957;70:39-44.

Yang L, Xu M, Koo Y, He J, Poethig RS. Sugar promotes vegetative phase change in Arabidopsis thaliana by repressing the expression of MIR156A and MIR156C. Elife. 2013;2:e00260.

Yu S, Cao L, Zhou CM, Zhang TQ, Lian H, Sun Y, Wu J, Huang J, Wang G, Wang JW. Sugar is an endogenous cue for juvenile-to-adult phase transition in plants. Elife. 2013;2:e00269.

Venables WN, Ripley BD. Modern Applied Statistics with S. Fourth Edition. 2002;Springer, New York.

Wickham H. ggplot2: Elegant Graphics for Data Analysis. 2009;Springer-Verlag New York.

## Figure legends

**Figure 1: The heteroblastic series in 40 *Passiflora* species. A)** Notable examples of heteroblastic changes in leaf shape in the indicated *Passiflora* species. **B)** Examples of changes in leaf shape across the heteroblastic series of the 40 *Passiflora* species analyzed in this manuscript, grouped by class. Leaves are scaled such that leaves in the series have the same height. Silhouettes of the first ten leaves of the series are shown. Leaves are arranged from the first leaf (at the shoot base) onwards towards the shoot tip.

**Figure 2: Morphometric methods used to study heteroblastic changes in *Passiflora* leaf shape. A)** The 15 landmarks used for analysis. Left to right, landmark placement when the distal and proximal veins l) pinnately emerge from the midvein, m) both originate from the petiolar junction, or r) the proximal vein

bioRxiv preprint doi: https://doi.org/10.1101/067520; this version posted October 24, 2016. The copyright holder for this preprint (which was not certified by peer review) is the author/funder, who has granted bioRxiv a license to display the preprint in perpetuity. It is made available under aCC-BY-NC-ND 4.0 International license.

branches from the distal. **B)** Harmonic contributions to shape resulting from Elliptical Fourier Descriptor (EFD) analysis. The harmonic rank is arranged horizontally and the amplification factor vertically. **C)** For each heteroblastic node, the mean leaf as measured with landmarks in shown in black, whereas all landmark data for leaves from the node are depicted in semi-transparent blue. **D)** The average landmark leaf from node 1 is depicted in green and superimposed upon the averaged landmark leaves from other nodes depicted in magenta. **E)** Mean leaves calculated for each heteroblastic node from the harmonic series resulting from an Elliptical Fourier Descriptor (EFD) analysis of leaf contours. The mean contour of leaves from node 1 is depicted in green and the mean contour leaves from other nodes in magenta. **F)** Sub-areas of Procrustes-aligned landmark data calculated for each leaf. **G)** Overall allometric relationships for the square root of distal blade area (light green), proximal blade area (dark green), midvein area (light brown), and proximal vein area (dark brown) plotted against the square root of overall leaf area. All areas are calculated from Procrustes-aligned landmark data as indicated in F). Heteroblastic node position is numbered "1" starting from the shoot base. Note: for convenience to the reader, panels A) and B) are recapitulated in the companion manuscript (Chitwood and Otoni, 2016). Leaf depicting sub-areas shown in **Fig. 3** re-drawn here for convenience.

**Figure 3: Allometric changes in relative leaf areas in different *Passiflora* species.** For each species, the linear relationships between the square root of sub-areas (distal blade area, light green; proximal blade area, dark green; midvein area, light brown; and proximal vein area, dark brown) are plotted against the square root of total area for Procrustes-aligned landmark data. Fitted linear models are super-imposed with 95% confidence bands against data points. Mean leaf contours for each species are provided for reference, colored by class membership. Heteroblastic node position is numbered "1" starting from the shoot base. Leaf depicting sub-areas shown in **Fig. 2** re-drawn here for convenience.

bioRxiv preprint doi: https://doi.org/10.1101/067520; this version posted October 24, 2016. The copyright holder for this preprint (which was not certified by peer review) is the author/funder, who has granted bioRxiv a license to display the preprint in perpetuity. It is made available under aCC-BY-NC-ND 4.0 International license.

**Figure 4: Allometric changes in relative leaf areas across the heteroblastic series.** Same plots as in **Fig. 3** except colored by heteroblastic node. For some species, strong linear allometric changes across the heteroblastic leaf series are observed. Heteroblastic node color scheme: shoot base, black; middle shoot, orange; shoot tip, yellow. Heteroblastic node position is numbered "1" starting from the shoot base.

**Figure 5: Juvenile leaves are similar in shape across *Passiflora* species. A)** Heatmap showing the proportion of correctly assigned species from Linear Discriminant Analyses (LDAs) performed with both landmark and Elliptical Fourier Descriptor (EFD) data for each heteroblastic node. The average correct assignment across species is provided as well. Generally, the proportion of leaves correctly assigned to species increased with heteroblastic node number. Averaged contours of leaves from each species are provided for reference and colored by class. **B)** For each trait, the standard deviation across each heteroblastic node is shown. Traits are arranged by hierarchical clustering and groups corresponding to x and y coordinates of landmarks indicated. Proportion correctly assigned: low, black; middle, orange; high, yellow. Standard deviation: low, black; middle, orange; high, yellow. Class color scheme: class A, teal; class B, orange; class C, lavender; class D, magenta; class E, green; class F, yellow; class G, brown. Heteroblastic node position is numbered "1" starting from the shoot base.

**Figure 6: Traversal of the heteroblastic series through t-SNE space. A)** Graph of Dimension 2 vs. Dimension 1 of leaves, colored by class, in a t-Distributed Stochastic Neighbor Embedding (t-SNE) analysis. **B)** Same data as in A) except with arrows corresponding to the leaf series collected for each plant. The first node (towards the base of the shoot) is the arrow base and indicated with a hollow, black circle. The last node (towards the tip of the shoot) is the arrow head. Arrows are colored by species class. **C)** The same arrow data as in B) except that the base of all arrows have been translated to the origin of Dimension 2 vs. Dimension 1. Arrows are colored by

bioRxiv preprint doi: https://doi.org/10.1101/067520; this version posted October 24, 2016. The copyright holder for this preprint (which was not certified by peer review) is the author/funder, who has granted bioRxiv a license to display the preprint in perpetuity. It is made available under aCC-BY-NC-ND 4.0 International license.

species class. Class color scheme: class A, teal; class B, orange; class C, lavender; class D, magenta; class E, green; class F, yellow; class G, brown.

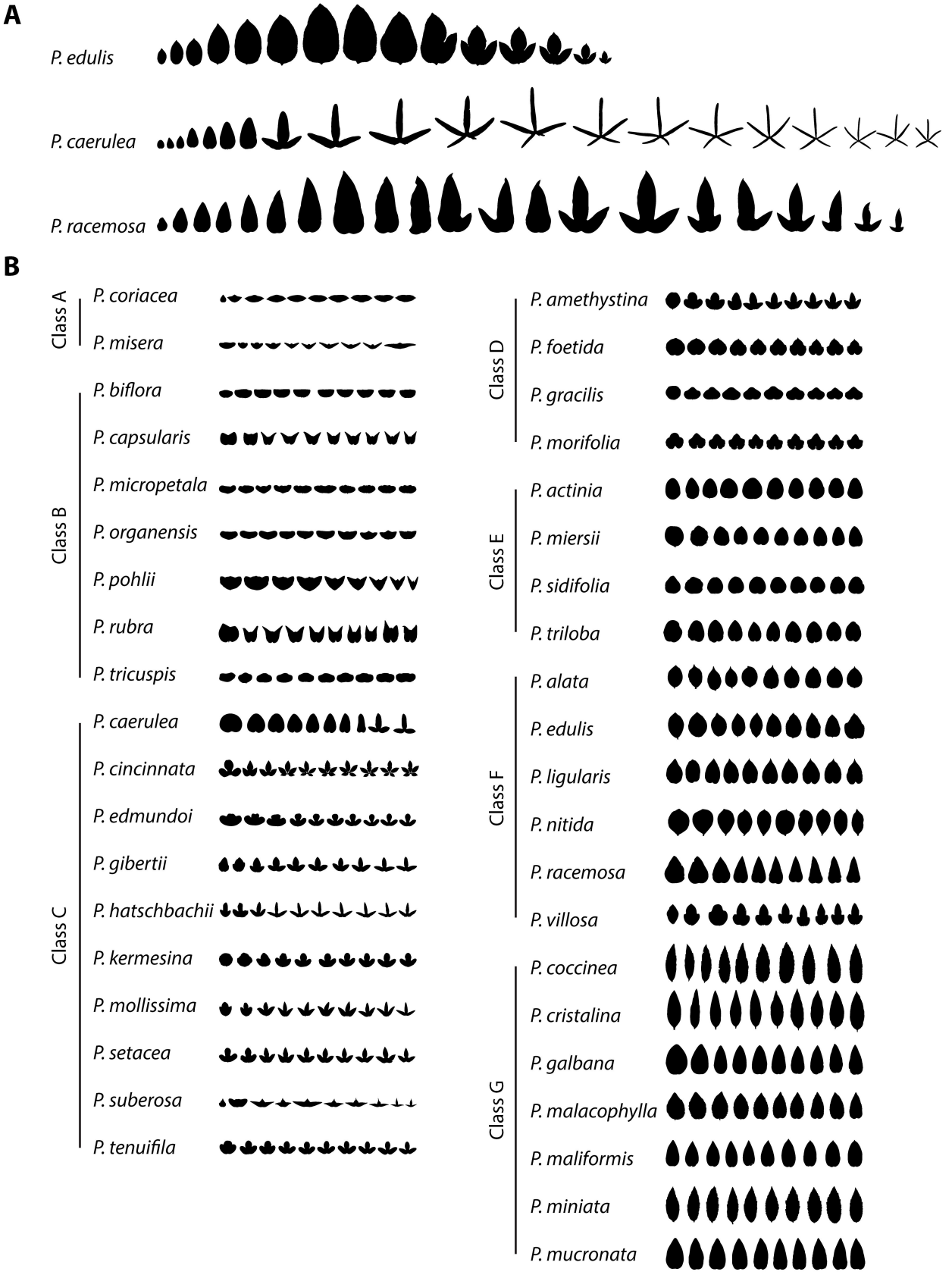
A
P. edulis
P. caerulea
P. racemosa
B
Class A
P. coriacea
P. misera
Class B
P. biflora
P. capsularis
P. micropetala
P. organensis
P. pohlii
P. rubra
P. tricuspis
Class C
P. caerulea
P. cincinnata
P. edmundoi
P. gibertii
P. hatschbachii
P. kermesina
P. mollissima
P. setacea
P. suberosa
P. tenuifila
Class D
P. amethystina
P. foetida
P. gracilis
P. morifolia
Class E
P. actinia
P. miersii
P. sidifolia
P. triloba
Class F
P. alata
P. edulis
P. ligularis
P. nitida
P. racemosa
P. villosa
Class G
P. coccinea
P. cristalina
P. galbana
P. malacophylla
P. maliformis
P. miniata
P. mucronata

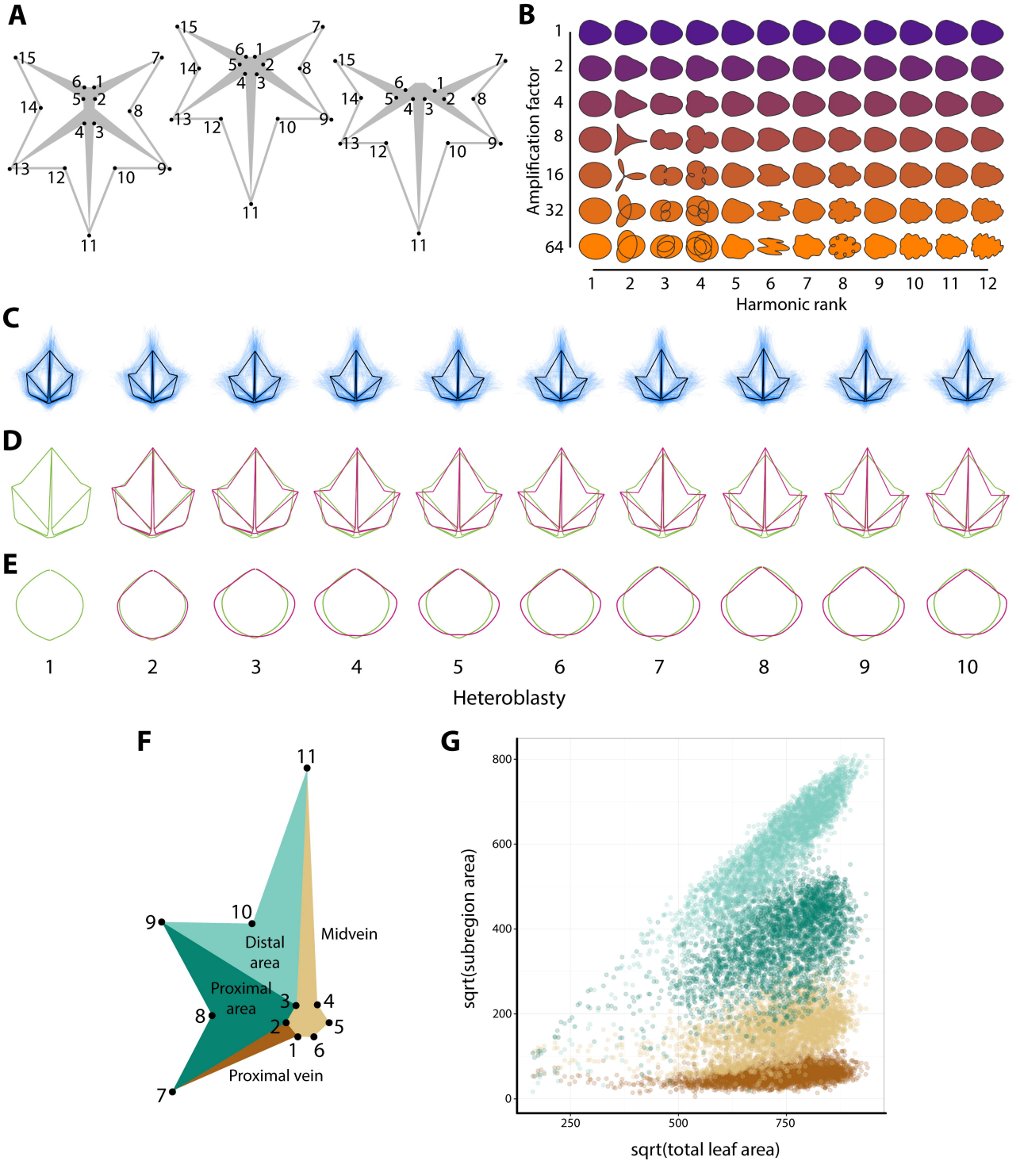
A
B
Amplification factor
1
2
4
8
16
32
64
Harmonic rank
1 2 3 4 5 6 7 8 9 10 11 12
C
D
E
1 2 3 4 5 6 7 8 9 10
Heteroblasty
F
Midvein
Distal area
Proximal area
Proximal vein
G
sqrt(subregion area)
sqrt(total leaf area)
0
200
400
600
800
250
500
750

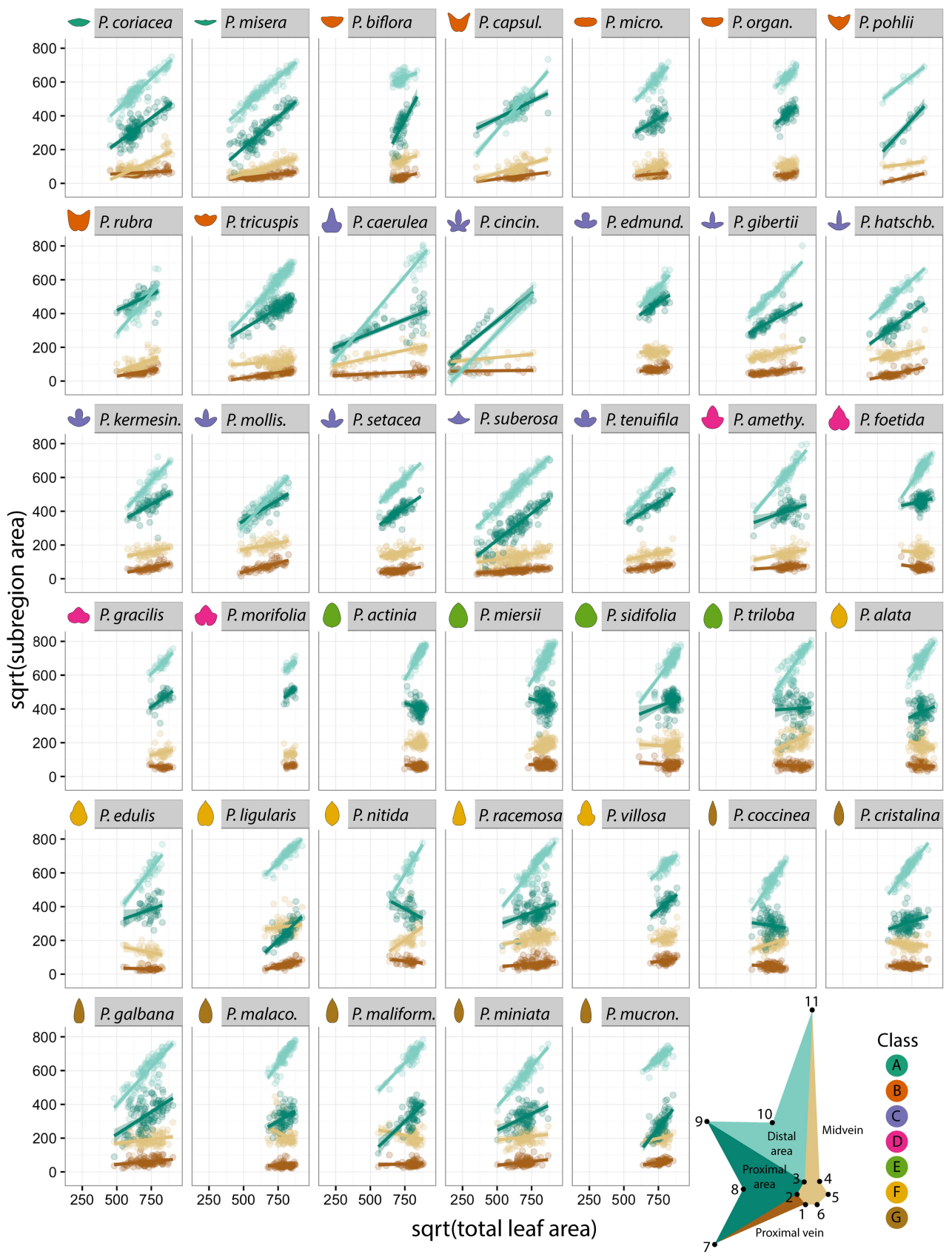
P. coriacea
P. misera
P. biflora
P. capsul.
P. micro.
P. organ.
P. pohlii
P. rubra
P. tricuspis
P. caerulea
P. cincin.
P. edmund.
P. gibertii
P. hatschb.
P. kermesin.
P. mollis.
P. setacea
P. suberosa
P. tenuifila
P. amethy.
P. foetida
P. gracilis
P. morifolia
P. actinia
P. miersii
P. sidifolia
P. triloba
P. alata
P. edulis
P. ligularis
P. nitida
P. racemosa
P. villosa
P. coccinea
P. cristalina
P. galbana
P. malaco.
P. maliform.
P. miniata
P. mucron.
sqrt(subregion area)
sqrt(total leaf area)
0
200
400
600
800
250
500
750
Class
A
B
C
D
E
F
G
Midvein
Distal area
Proximal area
Proximal vein
1
2
3
4
5
6
7
8
9
10
11

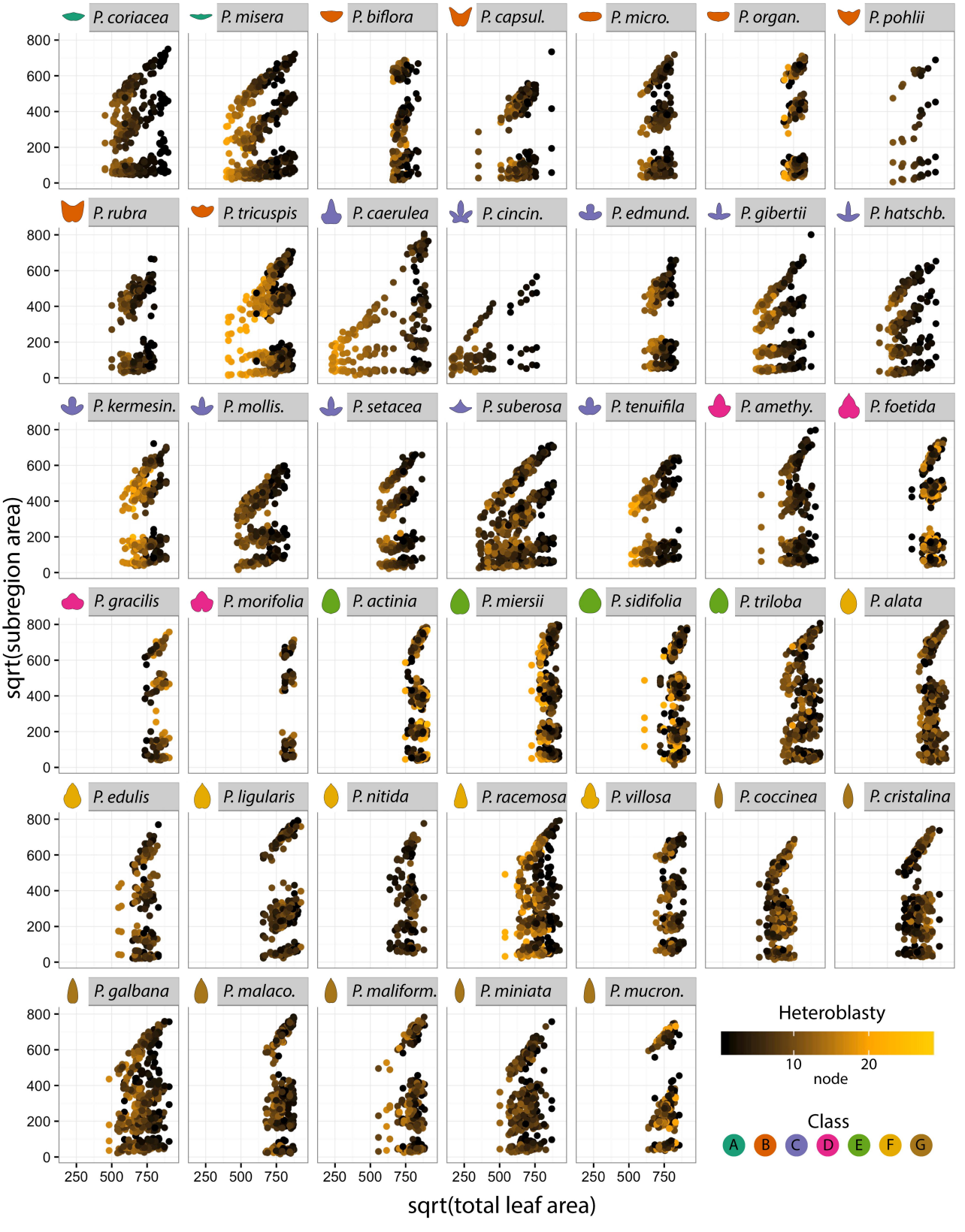
P. coriacea
P. misera
P. biflora
P. capsul.
P. micro.
P. organ.
P. pohlii
P. rubra
P. tricuspis
P. caerulea
P. cincin.
P. edmund.
P. gibertii
P. hatschb.
P. kermesin.
P. mollis.
P. setacea
P. suberosa
P. tenuifila
P. amethy.
P. foetida
P. gracilis
P. morifolia
P. actinia
P. miersii
P. sidifolia
P. triloba
P. alata
P. edulis
P. ligularis
P. nitida
P. racemosa
P. villosa
P. coccinea
P. cristalina
P. galbana
P. malaco.
P. maliform.
P. miniata
P. mucron.
sqrt(subregion area)
sqrt(total leaf area)
0
200
400
600
800
250
500
750
Heteroblasty
10
20
node
Class
A
B
C
D
E
F
G

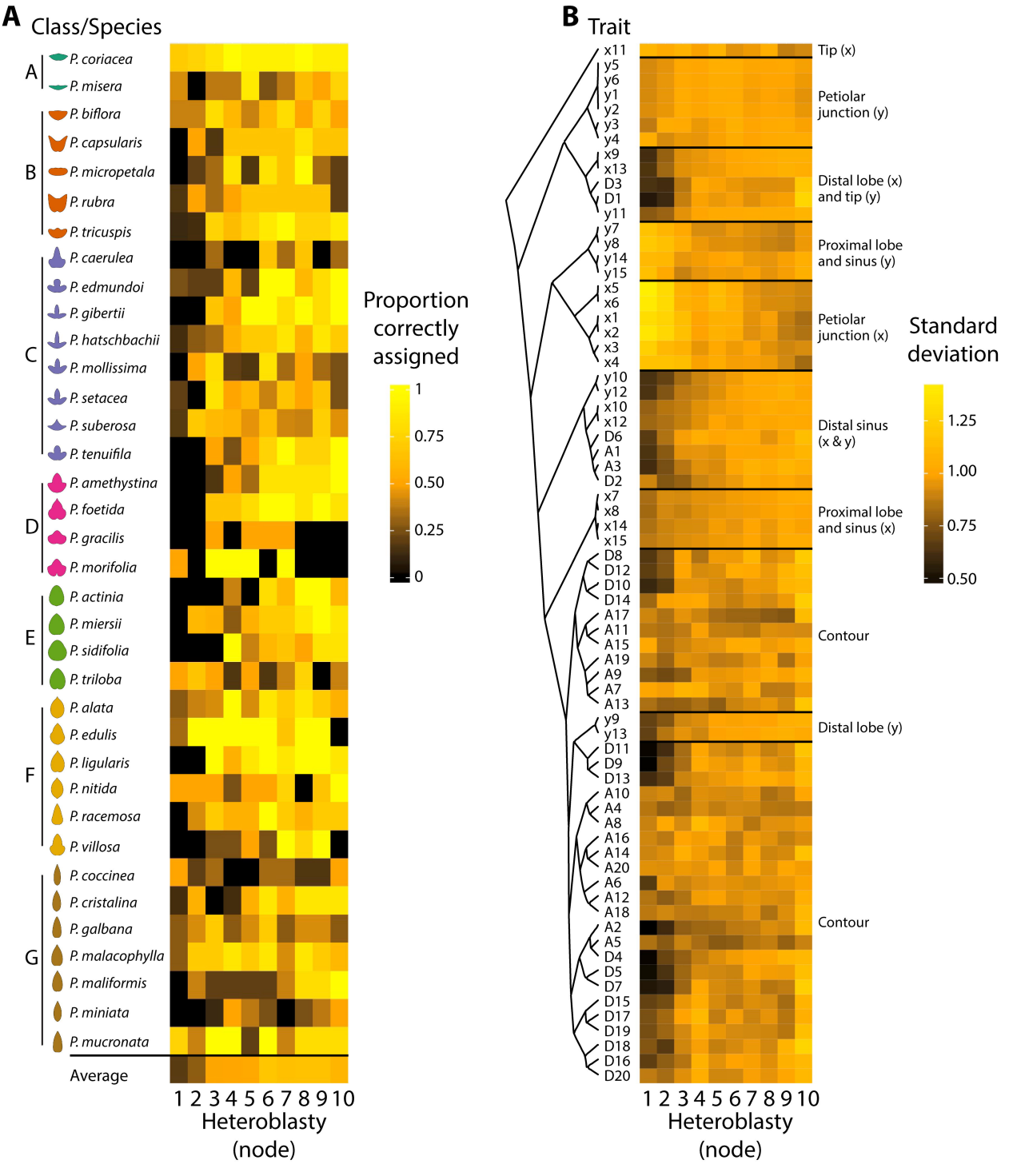
A
Class/Species
A
P. coriacea
P. misera
B
P. biflora
P. capsularis
P. micropetala
P. rubra
P. tricuspis
C
P. caerulea
P. edmundoi
P. gibertii
P. hatschbachii
P. mollissima
P. setacea
P. suberosa
P. tenuifila
D
P. amethystina
P. foetida
P. gracilis
P. morifolia
E
P. actinia
P. miersii
P. sidifolia
P. triloba
F
P. alata
P. edulis
P. ligularis
P. nitida
P. racemosa
P. villosa
G
P. coccinea
P. cristalina
P. galbana
P. malacophylla
P. maliformis
P. miniata
P. mucronata
Average
1 2 3 4 5 6 7 8 9 10
Heteroblasty
(node)
Proportion
correctly
assigned
1
0.75
0.50
0.25
0
B
Trait
x11
y5
y6
y1
y2
y3
y4
x9
x13
D3
D1
y11
y7
y8
y14
y15
x5
x6
x1
x2
x3
x4
y10
y12
x10
x12
D6
A1
A3
D2
x7
x8
x14
x15
D8
D12
D10
D14
A17
A11
A15
A19
A9
A7
A13
y9
y13
D11
D9
D13
A10
A4
A8
A16
A14
A20
A6
A12
A18
A2
A5
D4
D5
D7
D15
D17
D19
D18
D16
D20
Tip (x)
Petiolar
junction (y)
Distal lobe (x)
and tip (y)
Proximal lobe
and sinus (y)
Petiolar
junction (x)
Distal sinus
(x & y)
Proximal lobe
and sinus (x)
Contour
Distal lobe (y)
Contour
1 2 3 4 5 6 7 8 9 10
Heteroblasty
(node)
Standard
deviation
1.25
1.00
0.75
0.50

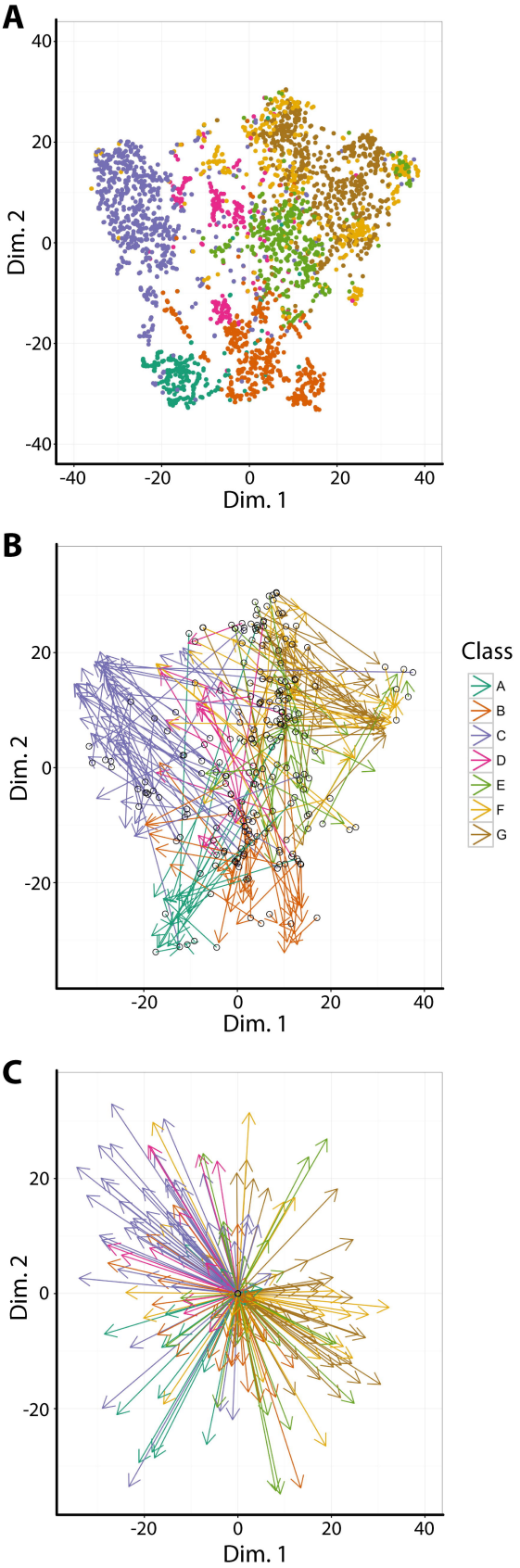
A
40
20
0
-20
-40
Dim. 2
-40
-20
0
20
40
Dim. 1
B
20
0
-20
Dim. 2
-20
0
20
40
Dim. 1
Class
A
B
C
D
E
F
G
C
20
0
-20
Dim. 2
-20
0
20
40
Dim. 1